

# Study of Impurity Transport Parallel to the Magnetic Field Lines with the Use of TPD-II

SUGIMOTO Tatsunori, MATSUBARA Akihiro<sup>1</sup>, SATO Kuninori<sup>1</sup> and SUDO Shigeru<sup>1</sup>

*Graduate University for Advanced Studies, Toki, 509-5292, Japan*

<sup>1</sup>*National Institute for Fusion Science, Toki, 509-5292, Japan*

(Received: 9 December 2003 / Accepted: 27 April 2004)

## Abstract

Impurity transport phenomena around the divertor target were studied experimentally. We simulated the impurity backflow from the divertor target making use of the linear plasma device and analyzed with a simple one-dimensional fluid modeling. Taking into account the thermal force with the ion temperature gradient of a several eV per meter, the calculated result explains well the observed spatial density distributions of impurity ions.

## Keywords:

divertor, impurity transport, carbon, linear machine

## 1. Introduction

In a divertor, the magnetic field lines are arranged to exhaust the escaping plasma into a separate place where it can be neutralized. This divertor configuration further improves the plasma purity. However, in the case that the divertor plasma attaches a divertor plates, the backflow of material from the divertor target is predicted. So, it is important to understand the impurity transport phenomena around the divertor target for the impurity control. In large fusion experiment devices (such as JT-60U, DIII-D, ASDEX), impurity transport in the divertor region has been investigated by measuring the impurity density and its flow velocity spectroscopically [1-5], and studied by the code including many processes such as the friction between impurities and background particles and temperature gradients [6-8]. However, it has not been clear how individual physical processes affect the impurity backflow.

By observing the spatial intensity distributions of carbon line emissions around the graphite target, we simulated experimentally the impurity backflow from the divertor target making use of the linear plasma machine called TPD-II and analyzed with a simple one-dimensional (1-D) fluid modeling.

## 2. Experimental setup and results

The experiments were carried out in the TPD-II (Test Plasma by Direct current discharge) linear plasma device. Figure 1 shows the setup for the experiments. TPD-II produces a steady quiescent state high-density plasma with a discharge current of 50 ~ 120 A, discharge voltages of 120 ~ 150 V, a magnetic field of ~2 kG. The cathode is composed

of Th-W pins and LaB<sub>6</sub> fragments. A discharge runs between the cathode and anode, and plasma flows out through a hole of anode. In case of helium discharge, the velocity of helium ion is  $10^3 \sim 10^4$  m/s toward the downstream side. The electron temperature  $T_e$  and density  $n_e$  were found to be several eV and  $10^{18} \sim 10^{19}$  m<sup>-3</sup> respectively. The neutral pressure in the plasma region is usually kept at less than 0.1 Pa.

To study the behavior of carbon sputtered at the graphite target, carbon emissions were observed with 0.5 m Czerny-Turner monochromator equipped with 2400-grooves/mm grating. The temperature of the carbon target was monitored with radiation thermometer.

Figure 2 shows the results of the spatial density distributions of carbon along the He plasma column, which are deduced from observed line intensities by using a corona excitation model. Here, the target position is set as the origin of the coordinate axes. The discharge current was varied between 70 ~ 80 A. In this case,  $T_e$  and  $n_e$  were observed about 8 eV and  $2 \sim 6 \times 10^{18}$  m<sup>-3</sup>, as measured by Langmuir probe (Fig. 3). We could observe the emissions from CI to CIII, which wavelengths are at 247.9 nm (CI), 283.4 nm (CII) and 229.7 nm (CIII). In front of the carbon target, strong spectral line of CI and CII were observed, and these spectral intensities decrease immediately toward the upstream side at about 0.6 m and 1.2 m from the target. The spectral line of CIII is observed about 2 m taking with the peak at about 1m from the target. At electron temperature of 8 eV, ionization rate coefficient of C<sup>+</sup> ion is  $\sim 10^{-9}$  cm<sup>3</sup>/s. Ionization relaxation time and penetration length of C<sup>+</sup> ion suggest the convection velocity of the order of  $\sim 10^3$  m/s.

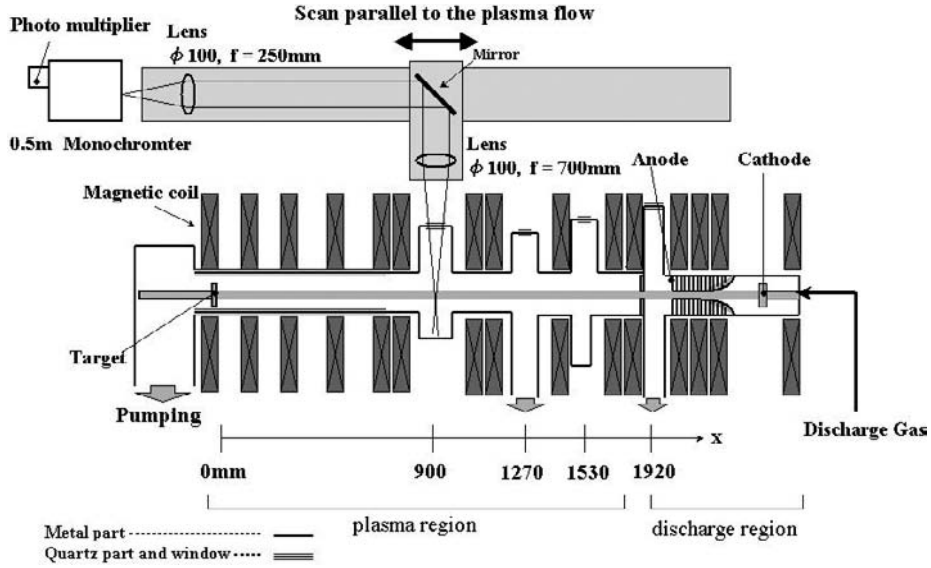


Fig. 1 Experimental setup for the TPD-II.

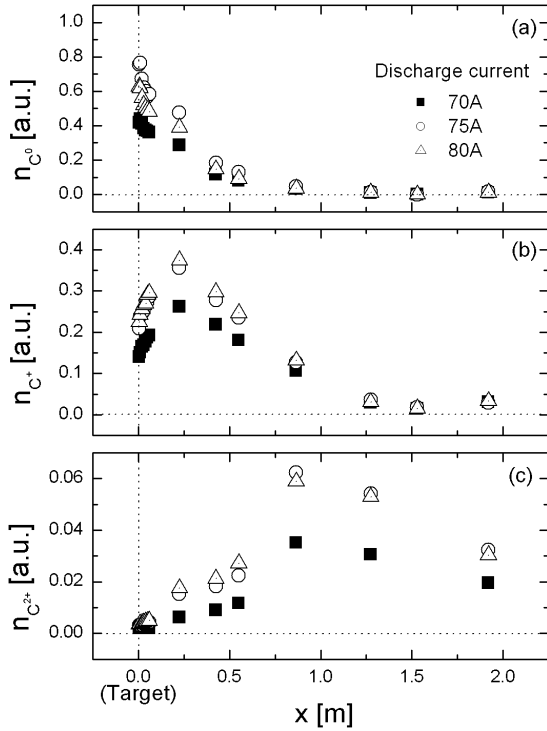
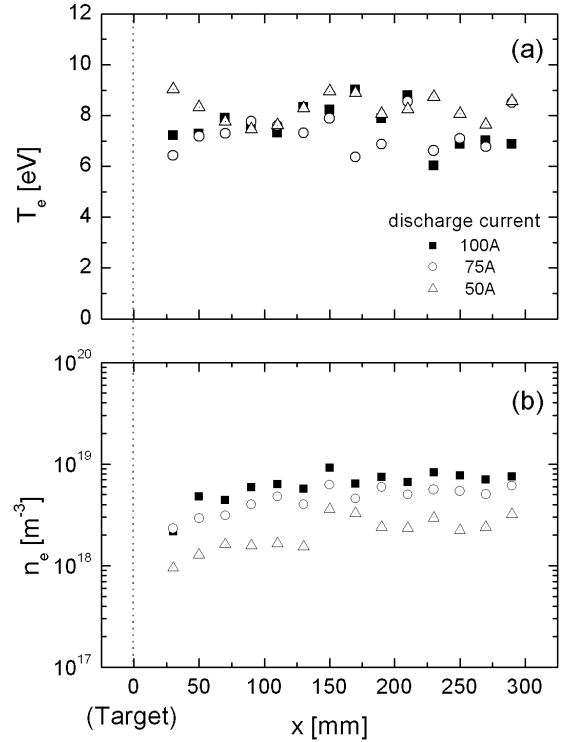

 Fig. 2 The observed spatial distributions of  $C^0$  (a),  $C^+$  (b) and  $C^{2+}$  (c).


Fig. 3 Axial profiles of electron temperature (a) and electron density (b) on the center of the plasma column and distance of 30 ~ 290 mm from the target measured by Langmuir probe

### 3. Impurity transport modeling and results

We used a 1-D fluid model to study impurity transport parallel to the magnetic field  $B$ . We assumed that the force on impurity ions of charge  $Z$  as [9]:

$$F_z = -\frac{1}{n_z} \frac{\partial P_z}{\partial x} + m_z v_{zi} (u_i - u_z) + ZeE + \alpha_z \frac{\partial kT_e}{\partial x} + \beta_z \frac{\partial kT_i}{\partial x} \quad (1)$$

where  $x$  is the distance measured from the target to the upstream direction, and the subscripts  $z$ ,  $i$  and  $e$  indicate the impurity, the helium ion as the background ion and the electron. The first term is the impurity pressure gradient force.  $n$  is density, and  $P$  is pressure. The second term is friction force on the impurity ions with velocity  $u_z$  exerted by the background ions moving with the velocity  $u_i$ .  $m$  is the mass, and  $v$  is the collision frequency, which assumed coulomb scattering

as:

$$v_{zi} = \frac{n_i Z^2 e^4}{4\pi m_z^2 \epsilon_0^2 v^3} \ln \Lambda \quad (2)$$

where  $\epsilon_0$  is the permittivity of free space, and  $\ln \Lambda$  is the coulomb logarithm.  $v$  is relative velocity between impurity and background plasma ion. Here, we considered the plasma is high temperature enough to neglect  $u_i$ . The third term is the electric force exerted by the parallel electric field  $E$ . The fourth and fifth terms are the background electron and the ion temperature gradient forces, where  $\alpha$  and  $\beta$  are coefficients both of order  $Z^2$ , and  $k$  is Boltzmann constant [10,11].

When the collision processes are strong enough in the plasma, the impurity ion flux is taken as:

$$\Gamma_z = -D_{\parallel z} \frac{\partial n_z}{\partial x} + V_z n_z \quad (3)$$

Here,  $D_{\parallel}$  is the impurity diffusion coefficient parallel to the magnetic field, and  $V$  is a convective velocity, and  $D_{\parallel}$  and  $V$  are taken as:

$$D_{\parallel z} = \frac{kT_z}{m_z v_{zi}} \quad (4)$$

$$V_z = \frac{1}{m_z v_{zi}} \left( -\frac{\partial kT_z}{\partial x} + ZeE + \alpha_z \frac{\partial kT_e}{\partial x} + \beta_z \frac{\partial kT_i}{\partial x} \right). \quad (5)$$

Similarly, we considered the impurity neutral flux. For neutral carbon, the effects of the electric force and the electron and ion temperature gradient forces can be neglected. Also, the collision process of between the impurity neutral and background ion is assumed a hard sphere collision.

The continuity equation for impurity can be written as:

$$\begin{aligned} \frac{\partial \Gamma_z}{\partial x} = & n_e n_{z-1} I_{z-1 \rightarrow z} - n_e n_z (I_{z \rightarrow z+1} + R_{z \rightarrow z-1}) \\ & + n_e n_{z+1} R_{z+1 \rightarrow z} - n_z \frac{D_{\perp z}}{\lambda_{\perp}^2}. \end{aligned} \quad (6)$$

Here,  $n_e$  is electron density, and  $I$  and  $R$  are the ionization and the recombination rate coefficient, which are a function of  $T_e$ .  $D_{\perp}$  is the impurity radial diffusion coefficient, where the classical diffusion coefficient is assumed. And a Bessel profile is assumed for the radial plasma density distribution with the radial diffusion scale length  $\lambda_{\perp} = r_0/2.405$ ,  $r_0$  is plasma radius. The charge exchange process was not taken into account in this continuity equation, since this process between the low ionized carbon ion and the helium neutral is assumed to be small in low temperature plasma compared to the ionization or recombination process and is neglected. We solved with the use of this continuity equations on  $C^0 \sim C^{3+}$  ( $C^0$ : neutral carbon).

When we calculated, we took a several assumption for simplification. a) The temperature of neutral carbon as an impurity source is assumed as the same as the target temperature. b) The carbon ion temperature is assumed as the same as the temperature of background helium ion, since the colli-

sion time between the carbon ion and the background ion is enough short about  $10^{-5}$  or  $10^{-6}$  s order. c) The parallel electric field in the plasma can be evaluated from the electron momentum balance equation [10], which can be written as:

$$E = -\frac{1}{en_e} \frac{\partial}{\partial x} (n_e kT_e) - 0.71 \frac{\partial kT_e}{\partial x}. \quad (7)$$

Firstly, we calculated the spatial distributions of carbon ions without the convection velocity on the transport. Figure 4 shows the calculated results. The each background plasma parameters are taken as  $T_e = 8$  eV,  $T_i = 2$  eV and  $n_e = n_i = 2 \times 10^{18} \text{ m}^{-3}$ . Also, we took the initial values of the impurity densities as  $C^0 = 1$  and  $C^+ \sim C^{3+} = 0$  on the target. The calculated result without the convective velocity shows the shifted spatial distribution toward the target side.

Secondly, we assumed that the ion temperature gradient is about a several eV per meter, since the temperature of ion near the discharge region should be higher than that of near the target. The calculated distributions, which include the convective velocity, get close to the observed ones (Fig. 5). This suggests that the small ion temperature gradient derives a large temperature gradient force. And resulted convective velocity of impurity ions affects the spatial distribution of impurity ions.

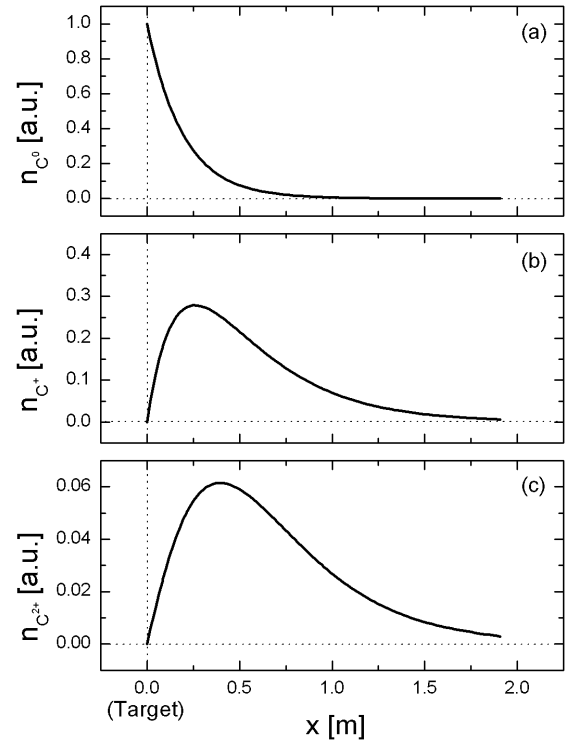


Fig. 4 The calculated results of the spatial distributions of  $C^0$  (a),  $C^+$  (b) and  $C^{2+}$  (c). Helium plasma parameters are taken as  $T_e = 8$  eV,  $T_i = 2$  eV,  $n_e = n_i = 2 \times 10^{18} \text{ m}^{-3}$ .

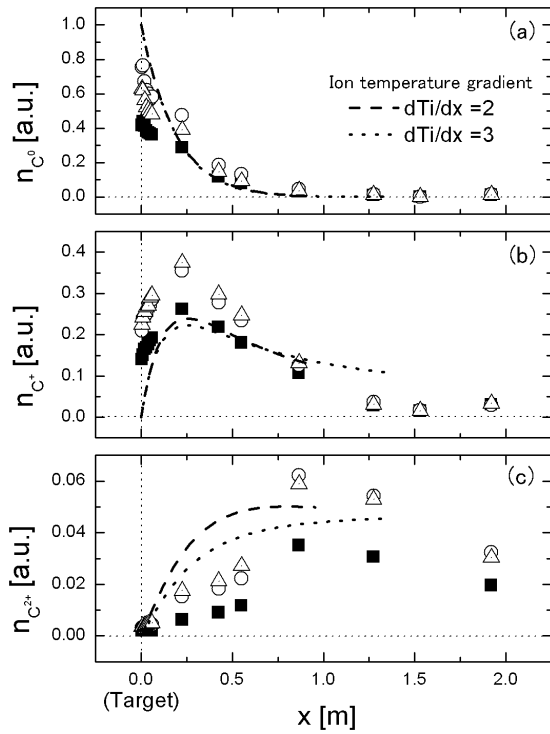


Fig. 5 The calculated spatial distributions of carbon, which include the ion temperature gradient force. Dashed line shows the case of the ion temperature gradient of 2 eV/m, dot line shows the case of the ion temperature gradient of 3 eV/m. Observed distributions are the same as Fig. 2.

#### 4. Summary

We simulated experimentally the impurity backflow from the divertor target using the linear plasma machine. Spatial intensity distributions of carbon emissions were measured in the helium plasma with graphite target. The calculated spatial distributions, which include the convective velocity of carbon ions, well explain the observed distributions. This suggests that the ion temperature gradient derives a large temperature gradient force. In the divertor region of fusion experiment devices, a large temperature gradient is expected. So, impurities produced at divertor target may flow into the core plasma by the temperature gradient force.

#### References

- [1] R.C. Isler *et al.*, Phys. Plasmas **6**, 541 (1999).
- [2] G.D. Porter *et al.*, Phys. Plasmas **7**, 3663 (2000).
- [3] B. Zaniol *et al.*, Phys. Plasmas **8**, 4386 (2001).
- [4] R.C. Isler *et al.*, Phys. Plasmas **8**, 4470 (2001).
- [5] R. Pugno *et al.*, J. Nucl. Mater. **290-293**, 308 (2001).
- [6] K. Shimizu *et al.*, J. Nucl. Mater. **220-222**, 410 (1995).
- [7] E. Haddad *et al.*, J. Nucl. Mater. **278**, 111 (2000).
- [8] W.P. West *et al.*, J. Nucl. Mater. **290-293**, 783 (2001).
- [9] P.C. Stangeby *et al.*, Nucl. Fusion **35**, 1391 (1995).
- [10] S.I. Braginskii, *Review of Plasma Physics*, edited by M.A. Leontovich (Consultants Bureau, New York, 1965) Vol. 1, p. 205.
- [11] S. Chapman, Proc. Phys. Soc. **72**, 353 (1958).